EXPLORATIVE STUDY INTO A SIMPLIFIED NUMERICAL EVALUATION OF THE BENDING CAPACITY OF REBAR REINFORCED STEEL FIBRE REINFORCED CONCRETE BEAMS DURING FIRE EXPOSURE

Xiliang NING[a, b, c], Van Ruben COILE[c], Luc TAERWE[c, d]*

[a] School of Architecture and Civil Engineering, Northeast Electric Power University, Jilin 132012, China
[b] State Key Laboratory of Green Building Materials, Bejing 100024, China
[c] Department of Structural Engineering, Ghent University, Ghent 9052, Belgium
[d] National RPGE Chair Professor, Tongji University, Shanghai 200092, China

Abstract

A simplified 2D numerical model for evaluating the bending capacity of rebar reinforced steel fibre reinforced concrete (R/SFRC) beams during fire is presented. Distinct material properties of steel fibre reinforced concrete (SFRC) and reinforcing steel bars are considered. The SFRC is treated as a homogeneous concrete "composite" which combines the advantages of the compression capacity of concrete and the tension capacity of fibre elements. Three steps are associated with the numerical model for evaluating the fire resistance of R/SFRC beams. Firstly, a fire temperature calculation. Secondly, thermal analysis evaluating the temperature inside the concrete cross-section in function of time. And finally, the structural analysis where the temperature dependent material properties are taken into account. The developed model for the bending capacity of R/SFRC beams is validated with test results, which demonstrates that the proposed numerical model captures the fire resistance of R/SFRC beams with reasonable accuracy.

Keywords: Steel fibre; beam; 2D numerical model; bending capacity; fire exposure

1 INTRODUCTION

Steel fibres are widely used in concrete structures to enhance the post-cracking behaviour of concrete. However, in the case of fire resistance design, the post-cracking tensile strength of SFRC is not taken into account by any current standard (EC2, 2004b; fib Model Code 2010, 2013). It is conservatively assumed that only the rebars carry tensile forces at elevated temperatures. This assumption is disadvantageous for the SFRC in determining the residual bearing capacity of a reinforced concrete member during fire, as the contribution of the fibres to the strength of the remaining cross-section after loading is neglected. Significant strength reserves may therefore be overlooked in the fire design process. In addition, there have been limited studies on evaluating the fire performance of structural members made by steel fibre reinforced concrete and conventional reinforcement (Kahanji et al., 2016; Heek et al., 2018). Thus, there is need for reliable experimental data, mathematical models and design specifications for predicting the fire resistance of rebar reinforced steel fibre reinforced concrete beams or slabs.

In the present paper, a temperature-dependent numerical model for the analysis of fire resistance of R/SFRC beam is presented. In order to obtain the bending capacity of a R/SFRC beam under high temperature, the following steps should be followed (i) fire temperature calculation, (ii) temperature distribution calculation over the cross section of the R/SFRC beam, and (iii) calculation of moment-curvature (M-χ) curves for tracing the structural response of the beam. In addition, after obtaining the moment-curvature (M-χ) curves, mid-span deflections of the beam at elevated temperature can be calculated based on the principle of virtual work.

2 MODELLING MATERIAL PROPERTIES OF SFRC AT ELEVATED TEMPERATURE

The fire resistance of R/SFRC beams exposed to fire depends strongly on the material properties of both SFRC and reinforcing steel. The modelling of the material properties of SFRC in the present

numerical model is discussed in this section. The mechanical properties of steel reinforcement at elevated temperature according to the EC2 (2004b) are used.

2.1 Stress-strain relations of SFRC

The discrete crack-bridging ability of fibres in fire is captured in a smeared way introducing a modified stress–strain relation according to fib Model Code 2010 (2013). The stress−strain relation of SFRC in tension used in the present model is given below:

$$\sigma_t = \begin{cases} k_E \cdot E_{fc} \cdot \varepsilon_t, & 0 \le \varepsilon_t \le \varepsilon_{tp} \\ k_{ft} \cdot \left[f_{Fts} + \left(f_{Ftu} - f_{Fts} \right) \cdot \left(\varepsilon_t - \varepsilon_{SLS} \right) / \left(\varepsilon_{ULS} - \varepsilon_{SLS} \right) \right], & \varepsilon_{tp} < \varepsilon_t \le \varepsilon_u \end{cases} \quad (1)$$

where f_{ft}, E_{fc} denote the tensile strength and modulus of SFRC at ambient temperature, respectively; $k_t(\theta)$, $k_E(\theta)$ are retention coefficients illustrating the degradation of tensile strength and elastic modulus of SFRC at elevated temperature, respectively. Linear-elastic behaviour is assumed up to the tensile strength f_{ft} and a bi-linear model is used to model the fibre's post-cracking bearing capacity employing two residual tensile strength values f_{Fts} and f_{Ftu} at fixed strains ε_{SLS} and ε_{ULS}, respectively (fib Model Code 2010, 2013). Fig. 1 illustrates the stress–strain relations of SFRC in tension at elevated temperature used in the present model.

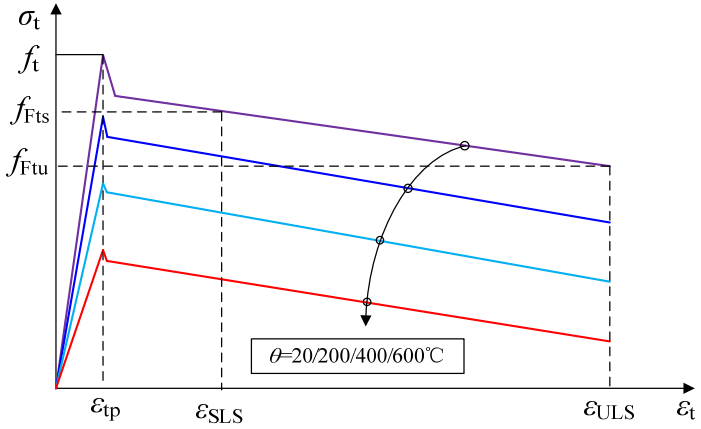

Fig. 1 Temperature-dependent stress-strain relations of SFRC in tension

The relative retention factors mentioned above rely on the local material temperature only:

$$k_t(\theta) = \begin{cases} 1.0, & 20℃ \le \theta \le 100℃ \\ 0.98 - 0.0005T - 5\times10^{-7}T^2, & 100℃ < \theta \le 800℃ \end{cases} \quad (2)$$

$$k_E(\theta) = \begin{cases} 1.0, & 20℃ \le \theta \le 100℃ \\ 1.1344 - 0.0017T + 5\times10^{-7}T^2, & 100℃ < \theta \le 800℃ \end{cases} \quad (3)$$

It is proposed as a conservative, bilinear function according to Eqs. (2) and (3) evaluated from literature data (Aslani et al., 2014). Degradation starts when θ exceeds 100 °C approximately and continues up to θ = 800 °C. Beyond, no tensile capacity is assumed.

3 NUMERICAL MODEL

In order to analyze the fire resistance of R/SFRC beams at elevated temperature, a simplified two dimensional numerical model is developed in this paper. There are mainly three steps, namely, fire temperature calculation, heat transfer analysis, and strength analysis.

3.1 Fire temperature calculation

Fire temperatures assumed to expose to three sides of the beams follow the standard fire such as ISO 834 (1999) or any other design fire scenario (EC2, 2004b). The temperature–time relationship for the ISO 834 standard fire can be approximated by the following equation:

$$T_f = T_0 + 345\log_{10}^{(8t_E+1)} \quad (4)$$

where t_E, time ,min; T_0, ambient temperature, °C; and T_f, fire temperature, °C.

3.2 Heat transfer analysis

The time-dependent distribution of the temperature gradient in an R/SFRC beam is described by Fourier's differential equation for heat conduction (Welty et al., 2001):

$$k\nabla^2 T = \rho c \frac{\partial T}{\partial t} \tag{5}$$

where k, ρ and c denote the temperature-dependent thermal conductivity, density and specific heat capacity, respectively. Steel reinforcement and steel fibres are assumed not to influence the temperature distribution, and consequently the reinforcement temperature is considered equal to the temperature of the concrete at the reinforcement axis position.

The heat flux to the outer surfaces of the R/SFRC beam via convection and radiation, is given by:

$$k\frac{\partial T}{\partial n} = h_c\left(T_f - T_m\right) + \sigma\varepsilon_m\varepsilon_f\left[\left(T_f + 273.15\right)^4 - \left(T_m + 273.15\right)^4\right] \tag{6}$$

where n denotes the outward normal direction of the beam surface; h_c is the thermal convection coefficient, W/(m^{2}K); T_f represents the fire temperature determined from the fire calculation above, °C; T_m is the surface temperature of the member, °C; ε_m denotes the surface emissivity of the member; ε_f is the emissivity of the fire; σ is the Stephan Boltzmann constant, W/(m^{2}K^4).

A thermal calculation tool similar to literature (Van Coile, 2015) is developed to numerically solve the differential equations by forward integration, using a time-discretization of 0.1 second and a cross-section discretization of 1 mm². A cross section of an R/SFRC beam and its discretization for the thermal analysis are shown in Fig. 2.

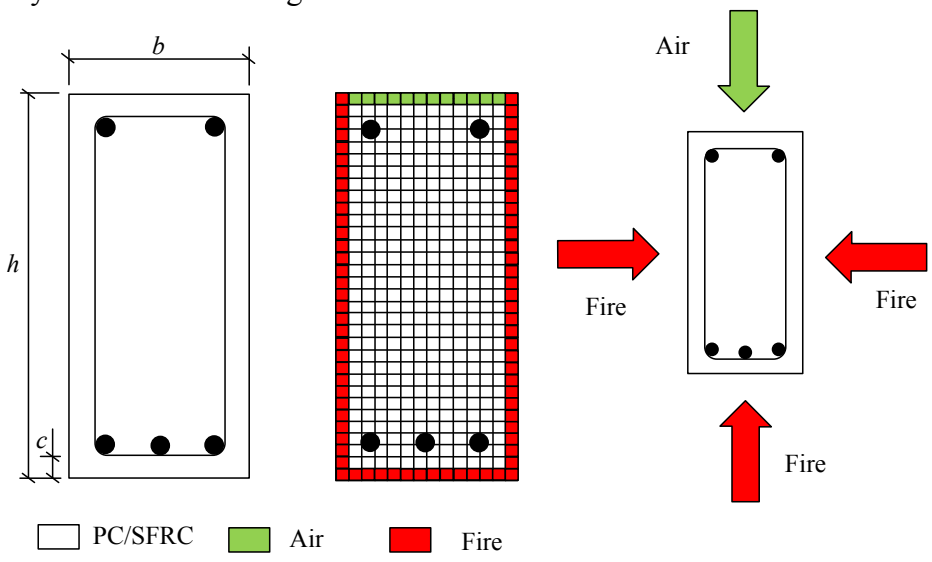

Fig. 2 Cross-section of an SFRC beam and its discretization for thermal analysis

3.3 Strength analysis

Regarding to strength analysis, the cross sectional temperature field generated from heat transfer analysis and the temperature-dependent stress–strain relations of SFRC in compression and tension are used as input. The strain relation in concrete and steel rebars can be written according to fib Bulletin 46 (2008) as:

$$\varepsilon_{tot} = \varepsilon_{mech} + \varepsilon_{th} \tag{7}$$

where ε_{tot} is the total strain, ε_{th} is the thermal strain, and ε_{mech} is the mechanical strain.

The strength calculations, at elevated temperatures, are carried out using the same rectangular network described above for the thermal analysis and shown in Fig. 2, which allows direct superposition of the thermal and mechanical portions of the strains according to Eq. (7). The temperatures, deformations and stresses in each element are represented by those at the centre of the

element. The temperature at the centre of the concrete element is obtained by averaging the temperatures of the nodes of that element in the mesh. The same procedure is used for steel reinforcement, where the values of stress, the strain components and temperature of each bar are represented by those at the centre of the rebar.
Mechanical modelling considers bending moments M and axial forces N only. Shear deformations are neglected. Plane sections remain plane after bending. Moreover, no slip between concrete and rebar is assumed. Post-cracking behaviour of SFRC, at elevated temperatures, is considered in the model based on the reduction factors proposed in literature (Aslani et al., 2014). Spalling of concrete is neglected. Applying equilibrium conditions for a two dimensional case yields:

$$N = \iint_A \sigma dA \cong \sum_A \sigma_c A_{ij} + \sum_{i=1}^{n} A_{si}\sigma_{si} \tag{8}$$

$$M = \iint_A \sigma z dA \cong \sum_A \sigma_c z_i A_{ij} + \sum_{i=1}^{n} A_{si}\sigma_{si} z_i \tag{9}$$

where σ_c represents stresses of SFRC, σ_{si} is the stress of the i^{th} steel rebar, A is the cross-sectional area, n denotes the number of steel rebars in the beam cross-section, A_{si} is the area of the i^{th} steel rebar, and z_i denotes the distance between the centre of the i^{th} element and the neutral axis of the beam. Iteration procedures are used to find the strain which satisfies the force equilibrium condition (e.g. N=0) at a specific curvature. Then the moment corresponding to the chosen curvature can be calculated using Eq. (9). Using the method mentioned above, we can obtain the moment-curvature relations of the beam at an arbitrary fire duration time.
After the sectional analysis of the beam mentioned above, the obtained moment-curvature curves are treated as input data for the calculation of the deflections of the beam based on the principle of virtual work. The general formula for concrete beams is given by:

$$f \cdot v = \int_L \left(N \cdot \varepsilon_{\text{mech}} + m \cdot \chi \right) dx \tag{10}$$

where, $\varepsilon_{\text{mech}} = f(N, M, t_{fire}, ...)$, strain caused by the mechanical load; $\chi = f(N, M, t_{fire}, ...)$, curvature caused by the mechanical load, vary with N, M, t_{fire}, etc.
In the case of a beam, N equals 0, so equation (10) can be written into:

$$f \cdot v = \int_L m \cdot \chi dx \tag{11}$$

where, f = 1N, the virtual force; $\chi = f\left(M\right)$, the moment-curvature relation at fire exposure time t_{fire}.
For discrete Δx_i, one obtains:

$$f \cdot v = \sum_i m_i \cdot \chi_i \left(M_i\right) \cdot \Delta x_i \tag{12}$$

By means of Eq. (12), we can calculate the deflection at an arbitrary point along the length of the beam at any time step.

4 VALIDATION OF THE NUMERICAL MODEL

There is insufficient research into the performance of reinforced steel fibre reinforced concrete beams at elevated temperature, as most studies have largely focussed on columns, slabs and smaller elements such as cubes and cylinders (Khaliq and Kodur, 2018).
Six beams tested under fire exposure by Kahanji et al. (2016) were selected and analyzed for validating the capability and accuracy of the present numerical model. Three of the beams contained steel fibres with a volume fraction of 2% and the other three had steel fibres with a volume fraction of 4%. All the beams were subjected to the ISO 834 standard fire (1999) and tested with fire exposure for 1 hour under three loading levels, i.e. 20, 40, and 60 percent of the ultimate strength of the beam at ambient temperature, as per EC2 (2004a) capacity calculation.
Six thermocouples in total were used to monitor the temperature distribution across the beams' depth and on the rebars. The locations of the thermocouples are illustrated in Fig. 3.

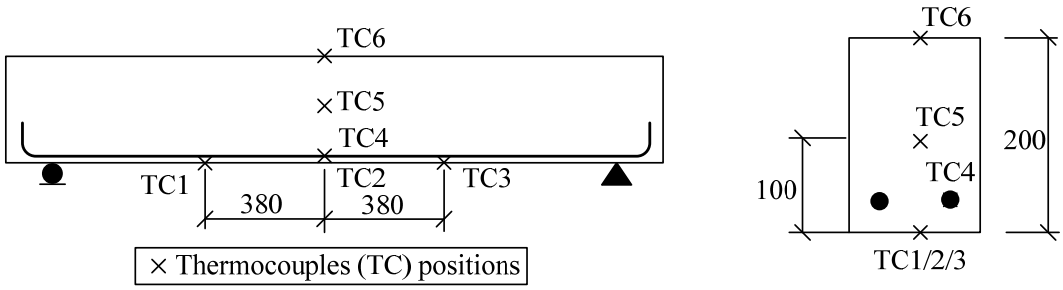

Fig. 3 Thermocouples positions

Fig. 4 shows the comparison of measured and predicted temperatures at various locations in beams RLF2-40 and RLF4-40. Close agreement is obtained. Moreover, it is interesting to note that peak temperatures in beams occur during the decay phase of the fire exposure. This can be attributed to thermal inertia of concrete, which leads to a lag between fire temperatures and the temperatures within a beam cross section. From Fig. 4, it can be seen that though different fibre volume fractions in beams RLF2-40 and RLF4-40, the temperatures at the positions of the rebars and the beam centre are nearly the same. The steel fibre volume fractions did not influence the thermal properties of the beam so much.

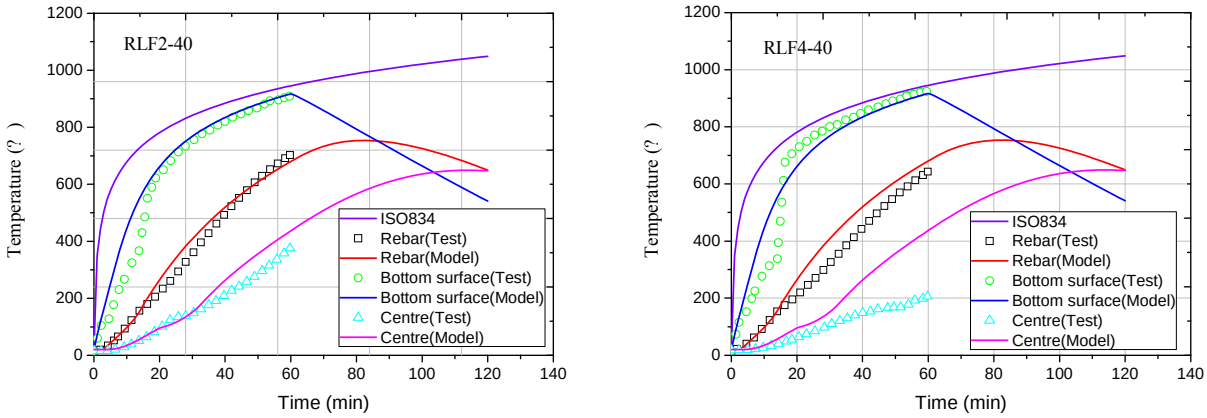

(a) RLF2-40 (b) RLF4-40

Fig. 4 Comparison of predicted and measured cross sectional temperatures during fire exposure

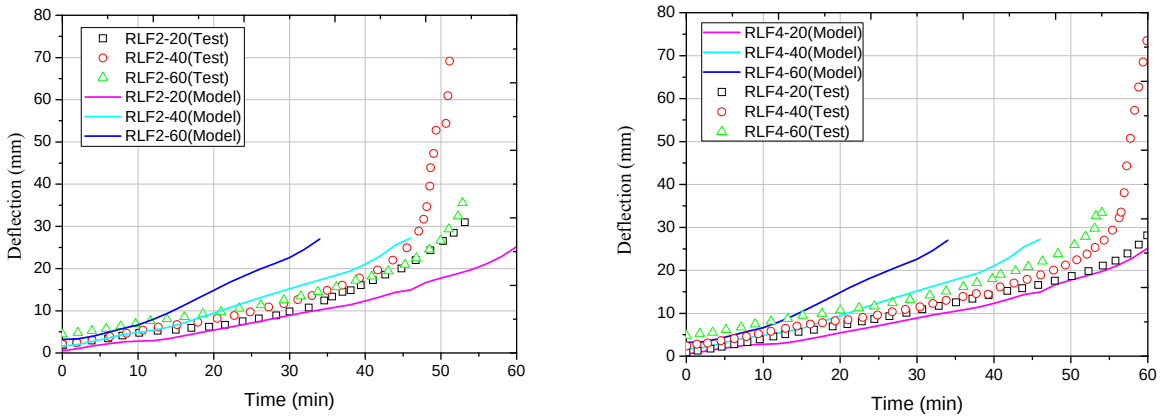

(a) RLF2 (b) RLF4

Fig. 5 Comparison of the predicted and measured mid-span deflections for beams during fire exposure

Fig. 5 illustrates the measured and predicted mid-span deflections of the beams during the fire. It can be seen that mid-span deflections increase during early stages of fire exposure due to degradation of strength and stiffness properties of SFRC and reinforcing steel with temperature. Since beams RLF2-40, RLF2-60, RLF4-40, and RLF4-60 were loaded with a relatively high load

ratio, all of them failed within 60 min of fire exposure. The beams RLF2-20 and RLF4-20 did not fail during the fire exposure period because of the lower load ratio. It can be seen from Fig. 8 that the predicted mid-span deflections agree well with the measured response during the fire test. However, for beams RLF2-60 and RLF4-60, earlier failures were found from the developed model than obtained in the tests. This may be due to the different fire exposure of the beam. Indeed, the tested beams were exposed to fire only over half the depth of the beam, while the developed model assumed that the full depth of the beam was exposed to fire.

5 CONCLUSIONS

Based on the results of the present research, the following conclusions can be drawn:

- Steel fibre contents did not influence the thermal properties of SFRC. Hence, the thermal properties for plain concrete can be used to calculate the temperature field of a beam section during fire exposure.
- Enhanced tensile behaviour of SFRC during fire exposure is observed from literature, and the modified fib Model Code model for the temperature-dependent stress-strain relation of SFRC in tension is applied, assuming a complete loss of tensile capacity above 800℃.
- The moment–curvature based 2D numerical model is capable of predicting the fire behaviour of R/SFRC beams, from the temperature distribution of the beam section to the deflection of the beam during fire exposure, with a good accuracy that is adequate for practical purposes.
- There is still limited information on the fire performance of R/SFRC beam, thus more validations for the structural behaviour of the beam, such as load–deflection relation of the beam after exposure to fire, should be carried out later.

ACKNOWLEDGMENTS

The authors gratefully acknowledge the National Natural Science Foundation of China (Grant: 51678100), the Special Foundation for Young Scientists of Jilin Province (Grant: 20190103048JH), Department of Education Science and Technology Project Funding of Jilin Province (Grant: JJKH20180423KJ), Project of the Chinese Scholarship Council (CSC) for the Youth Backbone Teachers Abroad Training, and the State Key Laboratory of Green Building Materials (YA-589).

REFERENCES

Aslani F., and Samali B., 2014. Constitutive relationships for steel fibre reinforced concrete at elevated temperatures. Fire Technology, 50(5): 1249-1268.

EN 1992-1-1, 2004a. Eurocode 2: Design of concrete structures - Part 1-1: General rules and rules for buildings.

EN1992-1-2, 2004b. Eurocode 2: Design of concrete structures. Part 1–2: General rules – Structural Fire Design. Commission of European Communities, Brussels.

Fib Bulletin 46, 2008. State-of-art report: Fire design of concrete structures–structural behaviour and assessment.

Fib Model Code 2010, 2013. Fédération internationale du béton / International Federation for Structural Concrete, Germany.

Heek P., Tkocz J., and Mark P., 2018. A thermo-mechanical model for SFRC beams or slabs at elevated temperatures. Materials and Structures, 51(4): 87.

ISO 834-1, 1999. Fire resistance tests – elements of building construction. Part 1:general requirement. Geneva: International Organization for Standardization.

Kahanji C., Ali F., and Nadjai A., 2016. Explosive spalling of ultra-high performance fibre reinforced concrete beams under fire. Journal of Structural Fire Engineering, 2016, 7(4): 328-348.

Khaliq W., and Kodur V., 2018. Effectiveness of Polypropylene and Steel Fibers in Enhancing Fire Resistance of High-Strength Concrete Columns. Journal of Structural Engineering, 144(3):04017224.

Van Coile R., 2015. Reliability-based decision making for concrete elements exposed to fire. PhD dissertation, Ghent University.

Welty J. R., Wicks C. E., Wilson R. E., et al., 2001. Fundamentals of Momentum, Heat, and Mass Transfer (4th edition). John Wiley & Sons, New York.